

# AUTOMATIC DATA PROCESSING FOR VISUALISING YAP AND PALAU TRENCHES BY GENERIC MAPPING TOOLS

Polina LEMENKOVA

## Automatic data processing for visualising Yap and Palau Trenches by Generic Mapping Tools

**Abstract:** Current research focus on using Generic Mapping Tools (GMT) cartographic scripting toolset for geodata processing aimed to visualize and compare geomorphic cross-section profiles of two trenches. Study area: Yap Trench (YT) and Palau Trench (PT), two hadal trenches located in south-west Pacific Ocean. Study aim: to do automatic geomorphological modelling by digitizing profiles in a fast and precise way. This was possible using GMT based automatic data processing through modules: “grdtrack”, “psxy” and “convert”. The methodology consisted in extracting raster dataset from the SRTM15\_PLUS, automated digitizing of the cross-sectional profiles on the selected segments, plotting profiles graphs for two trenches and statistical analysis on the bathymetry showing depth distribution. The results are the following. YT reaches -7,000 m, PT -6,200 m, that means that PT is shallower. YT has more abrupt slope and steep gradient of the profiles oceanward comparing to PT. For the diapason of -7000 m to -6000 m YT has 68 samples, while PT has 34 samples. PT has more samples below -6000 m, but YT has dominating depths at deeper values. In general, PT has more gentle geomorphic slope land and oceanwards, while YT has steeper slopes and deeper records. Topographic profiles of the axis of the YT have sharp V-shape while PT has U-shape which indicates more flat bottom of the YT with thin sediment cover of the axis. Development of the machine learning explains the importance of the geodata automatization. Automated cross-sectioning by GMT is more accurate, fast and less error-prone comparing to the manual process of digitizing by hand in traditional GIS. This paper demonstrated a GMT based methodology for the geomorphic modelling that can be applied both for submarine and terrestrial areas in similar works. The paper contributes to the development of the cartographic methodologies.

**Keywords:** GMT, SRTM15\_PLUS, profile analysis, bathymetry, Yap Trench, Palau Trench, Pacific Ocean

## Introduction

Yap and Palau trenches are hadal trenches located in the Philippine Sea, northwards from the Papua-New Guinea and eastwards from the Philippines, west Pacific Ocean (Fig. 1). According to the IHO classification, trenches are “long narrow, characteristically very deep and asymmetrical depressions of the sea floor, with relatively steep sides” (IHO, 2008).

Yap Trench with the greatest depth at 8,292 m is about 700 km long and 50 km wide (Sato et al., 1997). It stretches from the trench axis to Yap islands arc with a “J” form (Lee, 2004). It is morphologically divided into the northern and southern segments with the boundary between two segments at 8°26'N (Fujiwara et al., 2000). The Palau Trench with the greatest depth at 8,080 m (situated in its southern part) has a straight shape of the geometric form, stretching from the south-west to the north-east (Fig. 1 and Fig. 6.), located within a square 133°–136°E and 6°–8°N, eastwards from the Yap islands. One of the most unique characteristics of the Palau Trench is its short distance (35 km) between the trench axis and the coast of the Palau Islands westwards (Kobayashi

---

Polina LEMENKOVA, MSc., Ocean University of China, College of Marine Geo-sciences. 238 Songling Rd., Laoshan, 266100, Qingdao, Shandong, China (P.R.C.), pauline.lemenkova@gmail.com

et al., 1997). The geology of the Palau Trench includes sequences of the serpentinized peridotite, basalt and limestone on its landward slope and a huge block of coral-reef limestones at depths of 4,900 m to 6,500 m (Kobayashi et al., 1997). The Palau Trench is connected with the Kyushu-Palau Ridge in the north and Ayu Trough in the south. Yap and Palau trenches are distinguished from the flat-bottomed Ayu trough by their more similar to V shape in the cross section.

Islands of Palau are located westwards to the Palau Trench are composed of volcanic rocks capped by coral reef limestone. This indicates that Palau Islands were located along the volcanic front earlier (Kobayashi et al., 1997). The tectonic situation of the Yap and Palau trenches is on the Philippine Sea Plate. The Philippine Sea Plate is completely surrounded by the convergent boundaries of the tectonic plates (Yeh et al., 2013). The tectonic settings of the Yap and Palau trenches present a complex region of the convergence among three tectonic plates: the Philippine Sea, the Pacific and the Caroline plates. Hence, Yap and Palau trenches belong to the subduction zones surrounding Philippine Sea Plate along its eastern boundary.

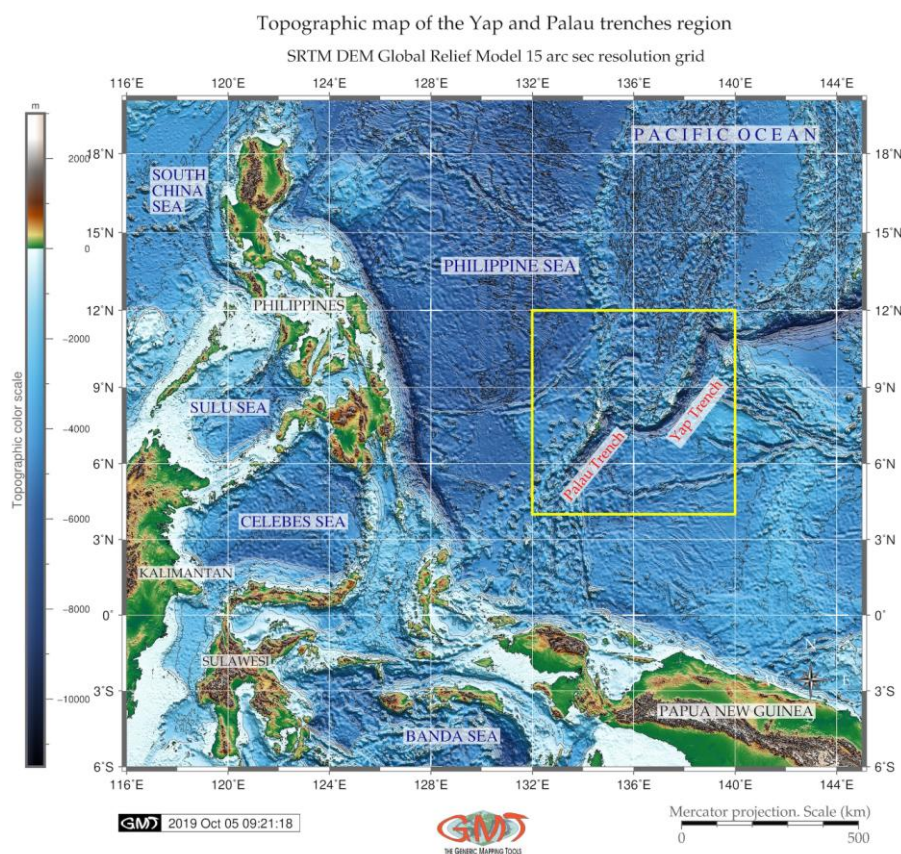


Fig. 1 Topographic map of the study area: Philippine Sea, Yap and Palau trenches.  
Figure source: author, made using GMT

The Yap-Palau subduction zone lies southwards off the Mariana arc-trench system. The Caroline plate subducts here north-westwards beneath the Philippine Sea Plate. The most prominent geological structures in the Caroline plate are the Caroline Ridge (Fig. 2), a buoyant oceanic plateau, and Sorol Trough, spreading in the middle of the ridge (Dong et al., 2018).

Yap and Palau trenches are formed in the place of the Philippine Sea Plate subduction and oceanic lithosphere sinking to the mantle. As sinking Philippine Sea Plate moves deeper into the mantle, the fluids are released from the mantle rock. This cause melting of the overlying mantle. The new magma (i.e. molten rock) rises to the surface and erupts violently forming volcanoes and arcs of islands along the convergent tectonic plate boundary. Therefore, earthquakes are common in the subduction zone of the Philippine Sea Plate (Fig. 2, red triangles on the map). Yap and Palau trenches form a typical trench-arc-basin system which includes deep trench, island arcs, and back-arc basin, a Parece Vela Basin, located in the eastern side of the Philippine Sea Plate (Fig. 2).

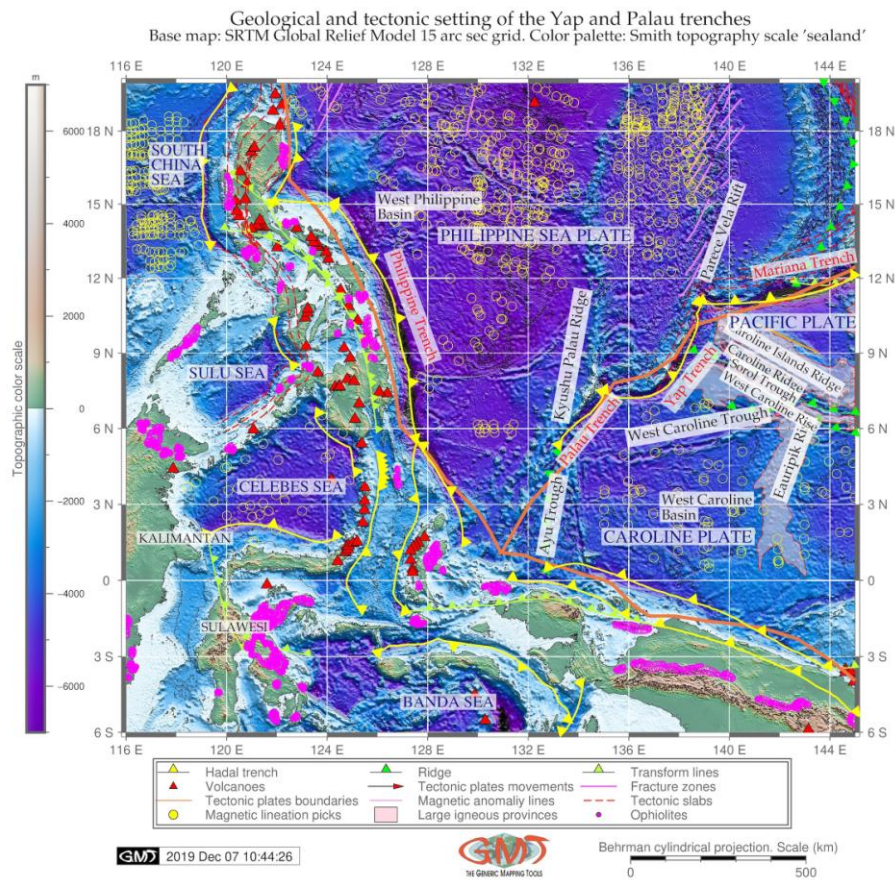


Fig. 2 Map of the geologic and tectonic settings: Yap and Palau trenches.  
Figure source: author, made using GMT

Such complex tectonic structure of the region is reflected in notable heterogeneity of the crustal and upper mantle velocity structures beneath the Philippine Sea Plate (Oda and Senna, 1982). Necessarily, it affects the submarine seafloor topography and its geomorphic shape. Further environment of Yap and Palau Trenches (e.g. biochemical and ecological setting) are well described in the relevant papers (Yang et al., 2018; Xu et al., 2018; Liu et al., 2018). Syntheses of the tectonic and magmatic evolution of the region of the Philippine Sea, Yap and Palau trenches can be found in further publications (Beccaluva et al., 1986; Pillet et al., 1999; Seton et al., 2012; Ohara et al., 2002; Tsuboi et al., 2011).

## 1. Methods

Methods of the mapping and modelling ocean seafloor is a high-level answer to the question: “How the geospatial data be best modelled and mapped to best visualize the submarine features, geographical phenomena and geological objects?” Correct methodology in data analysis aims at fast, precise and comprehensive data analysis with the high quality final output: maps, graphs, charts, diagrams. It furthermore provides a direct link between the cartographic goals and the technical possibilities of the selected GIS software.

General questions of the submarine geomorphic mapping and methodology have been presented and discussed in detail in various books chapters (e.g. Joseph, 2017; Owen, 2013; Oguchi, 2019). Excellent example of the World seafloor geomorphic mapping is presented by Harris (2012). Harris et al. (2014) reports the big project on global geomorphic seafloor mapping presenting the first global ocean seabed features map in digital format, based on the ArcGIS. Updated in electronic form, this project is based on all available datasets (Agapova, 1979), existing submarine geomorphic maps. Hence, it is a comprehensive map of the seabed physiography. Regional examples of the marine research include thematic maps (Suetova, 2005a), statistical data analysis (Lemenkova, 2018c), bathymetric swath cartography (Kuhn et al., 2006). Current paper is fully based on using Generic Mapping Toolset (GMT), a scripting cartographic toolset enable modelling and statistical analysis through scripting approach (similar to the programming codes). Unlike the traditional GIS, doing maps in GMT requires execution of the shell scripts. Each script consists of a set of codes used for visualizing cartographic elements, selecting projections, colour palettes, study areas, etc. Example of the GMT script is given further in chapter 2.3 Geomorphic modelling.

### 1.1 Data

Using high quality and fine resolution of topographic maps for the mapping is of utmost importance (Smith, 1993) since course resolution data will be prone to errors and lead to false modelling or misclassification of remote sensing data. The accuracy of input topographic data enables correct determination and visual distinguishing of the submarine geomorphic features: hadal trench axis, seamounts, canyons, basin characteristics etc. Originally, the Shuttle Radar Topography Mission (SRTM) was launched by NASA, USA. It is a mission from which exist several versions of DEMs, described technically in relevant papers (for example, Becker et al., 2009; Gesch et al., 2006a; Gesch et al., 2006b). SRTM15\_PLUS is a unique dataset, introduced in 2019 from the SRTM mission. Publicly available SRTM15\_PLUS dataset was used in the current research. Hence, the base map for this study is a high resolution (15 arc second) raster grid: a data fusion, SRTM15\_PLUS combining SRTM and other models for land and other datasets for bathymetry.

The SRTM Global Earth Relief Grids raster dataset (SRTM15\_PLUS) is the data fusion of SRTM and land topography with measured and estimated seafloor topography (NCEI Accession 0150537). Datasets are described more at official GMT webpage (GMT Datasets, 2019) or at the Satellite Group of Scripps Institution of Oceanography, 2019. The SRTM15\_PLUS used for this mapping was obtained using publicly available repository through the File Transfer Protocol (FTP): SRTM15\_PLUS DATASET (2019) as a netCDF4 grid tiles covering the Earth with the accuracy of 15 sec. It contains datasets used in the current research. The main file (topo15.grd) is an SRTM dataset. The original file obtained from the FTP is of 14.93 GB size and it covers the whole Earth. Any square can be cut using mask as it is done in this research.

The SRTM15\_PLUS tiles were made available to provide improvements to the surface water and ocean topography project to achieve the best possible measurements of an ocean surface slope for applications in marine geophysics, based on the publication: Olson et al. (2014), from the public directory of Scripps Institute of Oceanography: SRTM15\_PLUS DATASET (2019). The SRTM15\_PLUS is available in netCDF format. According to the description of the data resolution and range for the file grid used in this research (topo15.grd), it covers the Earth in the following extent and resolution in netCDF format derived from the full resolution shoreline: x\_min: -180 x\_max: 180; name: longitude [degrees\_east] nx: 86401; y\_min: -90 y\_max: 90; name: latitude [degrees\_north] ny: 43201; z\_min: -10927.5117188 z\_max: 8726 name: z; scale\_factor: 1 add\_offset: 0.

The dataset was prepared by masking necessary part from the initial grid using mask to cut a square by coordinates. Extracting a subset of SRTM15\_PLUS for the Yap and Palau trenches area was done technically using this GMT code: `grdcut topo15.grd -R116/145/-6/20 -Gypt_relief.nc`. Here `-R116/145/-6/20` options means the square with the coordinates West-East-South-North, in degrees. After that, the color palette was made for the SRTM15\_PLUS grid using this code: `gmt makecpt -Cgeo.cpt -V -T-11500/3000 > myocean.cpt`. At the next step the SRTM15\_PLUS grid for the selected area was physically visualized using `grdimage` module of GMT using this code: `gmt grdimage ypt_relief.nc -Cmyocean.cpt -R116/145/-6/20 -JM16c -P -I+a15+ne0.75 -Xc -K > $ps`.

The GEBCO Gazetteer of geographic names of the submarine features (IHO-IOC, 2012) was used to name features manually and to add them by hand where they are located (Fig. 1, Fig. 2). The coastline of the maps was taken from the embedded vector lines and polygons at GMT (Wessel and Smith, 1996).

Data used for a geoid and gravity were taken from the open repositories via the FTP: GEOID & GRAVITY DATASETS (2019): `geoid.egm96.grd` geoid grid based on the EGM96 geopotential model, on a 0.25×0.25 degree grid with respect to the WGS84 ellipsoid. Data were taken as available from the National Geospatial-Intelligence Agency (NGA NASA). The EGM96 is a spherical harmonic model of the Earth's gravitational potential. Using these data, Fig. 4 was modelled and mapped. Data of gravity grids were taken from the repositories of the Satellite Geodesy research group at Scripps Institution of Oceanography, University of California San Diego (Smith and Sandwell, 1995). According to the NOAA Documentation (2019), the ocean bathymetry is based on the bathymetric predictions from the latest global gravity model from CryoSat-2 and Jason-1 and depth soundings at 15 arc second resolution. The bathymetry grid with the improved gravity was used to construct a global seafloor map.

## 1.2 Geoid and gravity modelling

The geophysical aspect of the geoid and gravity maps can be briefly summarized as follows. Density variations of the Earth's interior cause geoid undulations, as well as gravity anomalies and gradient changes. Since geoid undulations cause gravity indirect effects (Chapman and Bordine, 1979), geoid and gravity have visual correlations between each other (Fig. 3, Fig. 4). Because the structure and submarine geomorphology of the ocean trench is affected by Earth's interior through tectonic plates subduction and movements, the visual shape of the geoid and gravity is distinctly repeating the isolines (Fig. 1, 3 and 4). The accuracy of the marine gravity measurements is important for reliable results and refines approximation of the models with Earth ellipsoid (Wessel and Watts, 1988).

## 1.3 Geomorphic modelling

The demand for the automatization of the cartographic processes requires updated methodologies of fast and precise digitizing routines through the machine learning approaches. Due to the wide variety of GIS software and diverse types and approaches of geodata processing, methods can be diverse and argued about the best solutions. Examples of the machine learning approaches in digitizing raster maps and converting them to the vector format in a semi-automated regime is presented by Schenke and Lemenkova (2008).

Current research presents the experience of the automatization of the cartographic data processing obtained using GMT scripting through the sequential GMT coding by modules `"grdtrack"`, `"psxy"` and `"convert"`. The main module is `"grdtrack"` which presents automatization of the data processing for cross-section transecting. Six profiles were plotted for the Palau Trench and seven for the Yap Trench (Fig. 6) using following GMT code sequence:

- Extracting a subset of the SRTM15\_PLUS for the Yap and Palau trenches: `grdcut topo15.grd -R132/140/4/12 -Gypts_relief.nc`
- Making color palette: `gmt makecpt -Cglobe -V -T-11000/2000 > myocean.cpt`

### Marine free-air gravity anomaly: Yap and Palau trenches area

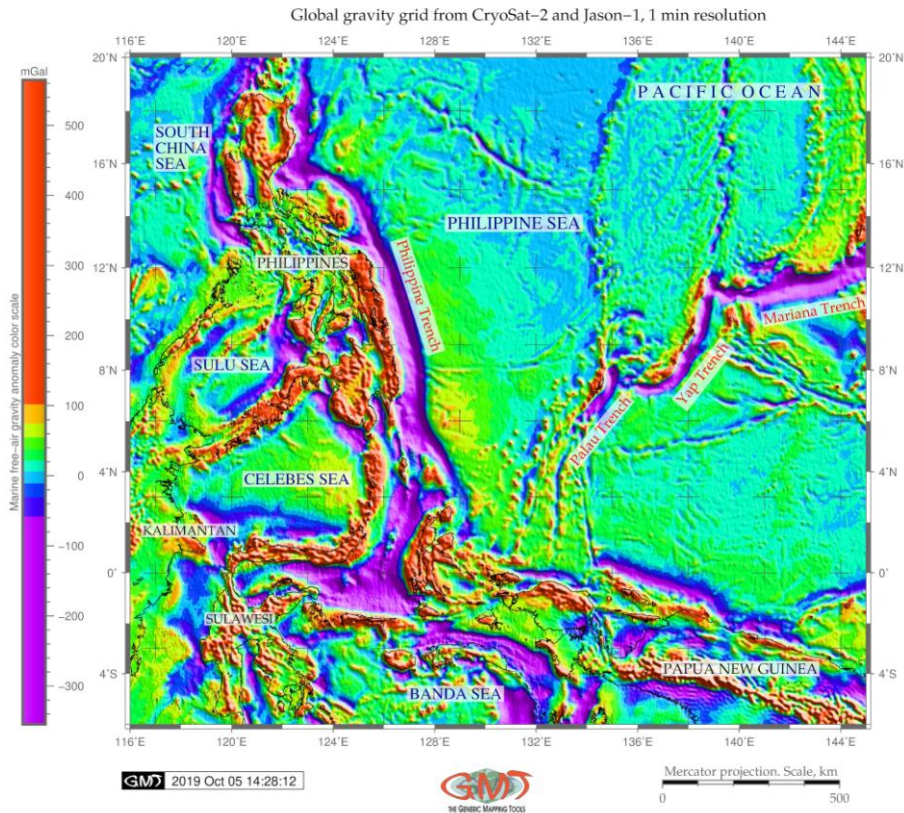


Fig. 3 Map of the free-air gravity anomaly, Yap and Palau trenches.  
Figure source: author, made using GMT

- Making raster image: `mt grdimage ypts_relief.nc -Cmyocean.cpt -R132/140/4/12 -JM16c -P -I+a15+ne0.75 -Xc -K > $ps`
- Adding color legend: `gmt psscale -Dg128.0/4+w11.0c/0.4c+v+o0.3/0i+ml -Gypts_relief.nc -J -Cmyocean.cpt -Baf+! "Color scale legend: depth and height elevations (m)" -I0.2 -By+lm -O -K >> $ps`
- Adding shorelines: `gmt grdcontour ypts_relief.nc -R -J -C1000 -B+t "Cross-sectional profiles of two trench segments: Yap (yellow) and Palau (red)" -W0.1p -O -K >> $ps`
- Adding cartographic grid: `gmt psbasemap -R -J -Lx13c/-1.2c+c50+w200k+! "Mercator Projection. Scale (km)" +f -Bpxg4f2a1 -Bpyg4f2a1 -Bsxg2 -Bsyg1 -UBL/-5p/-35p -O -K >> $ps`
- Adding text annotations: `gmt pstext -R -J -N -O -K -F+f12p,Times-Roman,black+jLB -Gwhite@20 -Wthinnest,darkbrown >> $ps << EOF 138.0 8.0 Yap Trench 133.8 6.0 Palau Trench EOF`
- Selecting two points for defining segment on the Yap Trench: `cat << EOF > trenchYT.txt 136.9 7.3 137.7 7.9 EOF`
- Plotting line: `gmt psxy -Rypts_relief.nc -J -W2p,yellow trenchYT.txt -O -K >> $ps`
- Plotting points: `gmt psxy -R -J -Sc0.15i -Gyellow trenchYT.txt -O -K >> $ps`
- Generating cross-track profiles 400 km long, spaced 20 km, sampled every 2 km: `gmt grdrack trenchRT.txt -Gpct_relief.nc -C400k/2k/20k+v -Sa+sstackPCTn.txt > tablePCTn.txt`
- Saving these data to the table: `gmt grdrack trenchYT.txt -Gypts_relief.nc -C400k/2k/20k -Sm+sstackYT.txt > tableYT.txt`

- Plotting profiles: `gmt psxy -R -J -Wthin, yellow tableYT.txt -O -K >> $ps`
- Showing upper/lower values encountered as an envelope: `gmt convert stackYT.txt -o0,5 > envYT.txt`  
`gmt convert stackYT.txt -o0,6 -I -T >> envYT.txt`

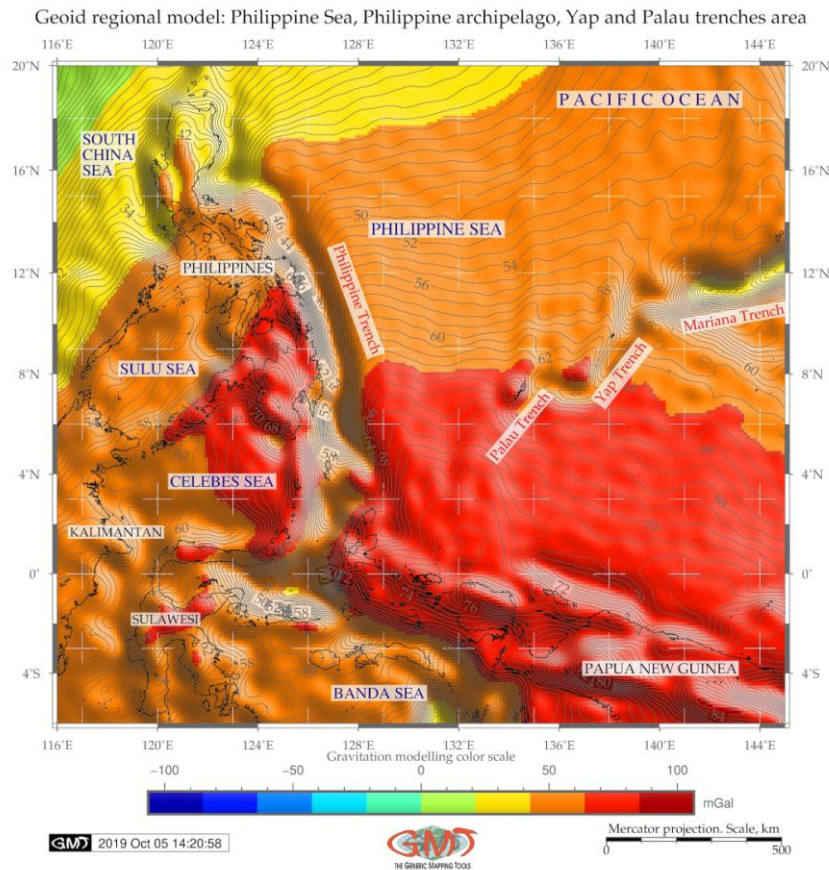


Fig. 4 Map of the geoid model, Yap and Palau trenches.  
Figure source: author, made using GMT

The presented above sequence of the GMT codes produces the automatically digitized profiles for the Yap Trench. The same procedure was repeated for the Palau Trench with changed coordinates of the starting and end points of the segment to '134.4°E 6.6°N 135.0°E 7.3°N'. Now profiles were drawn orthogonally, in a perpendicular direction to the trenches axis (Fig. 6). The next step included plotting graphs and comparing the two trenches (Fig. 7). The X axis on the Fig. 7 on the bottom of each graph indicates position of the axial profile. The red line on the graphs shows median calculated as a statistical median from the data pool.

The error bars associated with digitized profiles estimations for each trench profiles derived from the several profiles for each trench. These include spatial distribution and accuracy of the depth measurements used in creating the model of the profiles. On the plot (Fig. 6) they are shown as thin lines showing the range of the data. A detailed 3D mesh plot on top of the 2D geoid contour image as a block diagram was created as a combination of bathymetric and geoid image (Fig. 5).

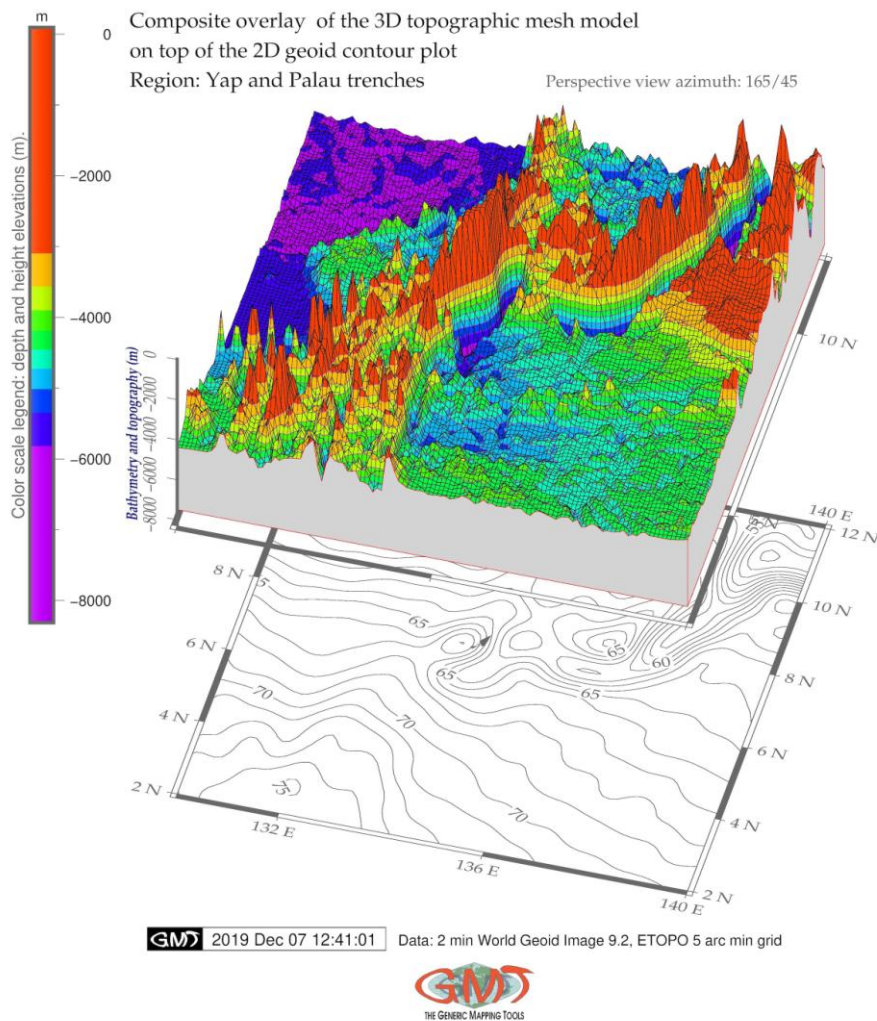


Fig. 5 Geomorphic 3D model of the Yap and Palau trenches.  
 Figure source: author, made using GMT

#### 1.4 Statistical analysis and graph plotting

Bathymetric samples taken from the digitizing were examined for frequency using the following code for plotting histograms (here is the example for the Palau Trench):

- gmt pshistogram tablePT.txt -i4 -R-8000/6/0/25 -JX4.8i/2.4i -X3.6i -Bpxg1000a1000f100+I"Bathymetry (m)" -Bpyg5a5f2.5+I"Frequency"+u" %" -Bsyg2.5 -BWSne+gsnow1 -Glightsteelblue1 -D+f7p,Times-Roman,black -L0.1p,dimgray -Z1 -W250 -N0+pred -N1+pblue -N2+pgreen -UBL/8.5c/-1.8c -K > \$ps
- UNIX 'echo' utility was used to plot annotations: echo "-7500 20 B" | gmt pstext -R -J -F+jBR+f15p,black -Gfloralwhite -W0.5p -O -K >> \$ps
- Next step is adding legend: gmt pslegend -R -J -Dx0.5/-3.0+w6.0c+o-1.0/0.5c -F+pthick+ithinner+gwhite -O -K << EOF >> \$ps S 0.3c - 0.8c - 0.5p,red 1.0c Mean and standard deviation S 0.3c - 0.8c - 0.5p,green 1.0c LMS mode and scale S 0.3c - 0.8c - 0.5p,blue 1.0c Median and L1 scale EOF



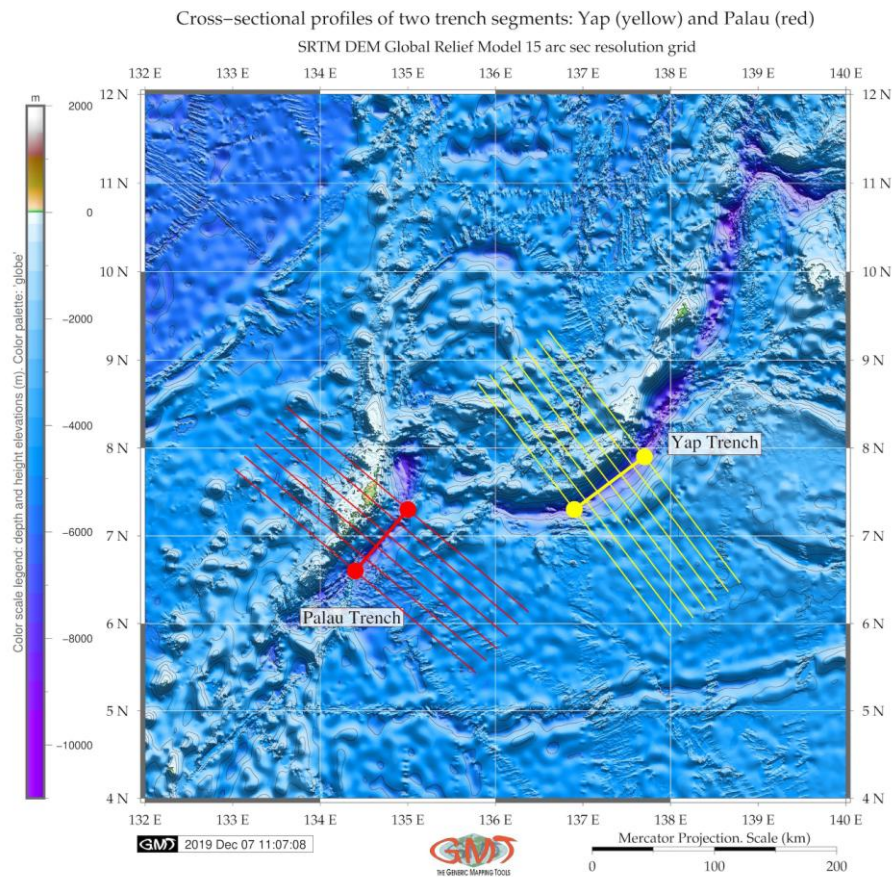


Fig. 6 Map of the digitized profiles, Yap and Palau trenches.  
Figure source: author, made using GMT

The statistical method of histograms for frequency data analysis was described in more details previously (Lemenkova, 2019b). It shows data distribution using binning data. At the next step, the trend curves of the gradient slopes were modelled using three different mathematical approximations aimed at visualization of the steepness of two trenches: Yap (Fig. 9) and Palau (Fig. 10).

## 2. Results

### 2.1 Results on geoid and gravity modelling

The free-air gravity anomalies reflect, in general, the bathymetry (compare Fig. 3 and Fig. 1). Comparing to the neighbouring Mariana Trench, the gravity field of the Yap and Palau trenches are narrower (purple coloured strip on the map). The free-air gravity values reach positive above 100 to 500 mGal (red colour) mostly over the area of Philippine Islands and small islands of the archipelago. Positive 70 to 100 mGal are notable over the shelf areas (orange colour on the map). The gravity over the basin of the Philippine Sea generally fluctuates between -20 to 0 mGal range (light blue colour) to 0–20 mGal (cyan). The characteristics of the gravity field mirrors relationship between the gravity anomaly and geoid undulation as determined by Haxby et al. (1983) for gravity anomalies from a grid of geoid undulations. The geoid model visualizing study area (Fig. 4) shows subdued isolines in the Yap and Palau trenches.

## 2.2 Results on geomorphic modelling

Comparing Yap and Palau trenches, the following findings can be reported. First, the Yap Trench reaches -7000 m in its median curve of the profiles, while the Palau Trench only -6200 m, that is the Palau Trench is shallower. Second, the Yap Trench has distinctly more abrupt slope and steep gradient of the profiles oceanward (Fig. 7B) comparing to the Palau Trench (Fig. 7A). Kobayashi et al. (1997) earlier pointed that extensive slope failure is occurring on the landward slope of the Palau Trench from which great amount of mass is wasted to the trench axis. Hence, if surface sediments or rocks are collapsed into the trench axis, the V-shaped bottom will be gradually buried to form a flat basin, unless subduction or the tectonic erosion proceeds. Submarine sediment avalanches occur easily and frequently, when dipping angles of the lower landward slope partly exceed slope failure limit. With this in view, the comparison of the graduate slopes is important (Fig. 9 for Yap Trench and Fig. 10 for Palau Trench). This can contribute to the explanation of the differences between two trenches in the geomorphic shape: as we can notice, inner slopes on the Yap Trench are more steep and abrupt (Fig. 7B) while the Palau Trench (Fig. 7A) has more gentle slope with sediment accumulation on the inner side. Fig. 7 shows modelled profiles of the bathymetry of the Palau (A) and Yap (B) trenches. The average dip of the landward slope is recognized as about  $29^\circ$  for the Yap Trench westwards  $41^\circ$  eastwards and while for the Palau Trench it is  $17^\circ$  westwards and  $18^\circ$  eastwards, respectively. The topography of the Palau Trench is more similar to an upside-down mound. Generally, the Yap Trench has abrupt shape with no marine terraces identified.

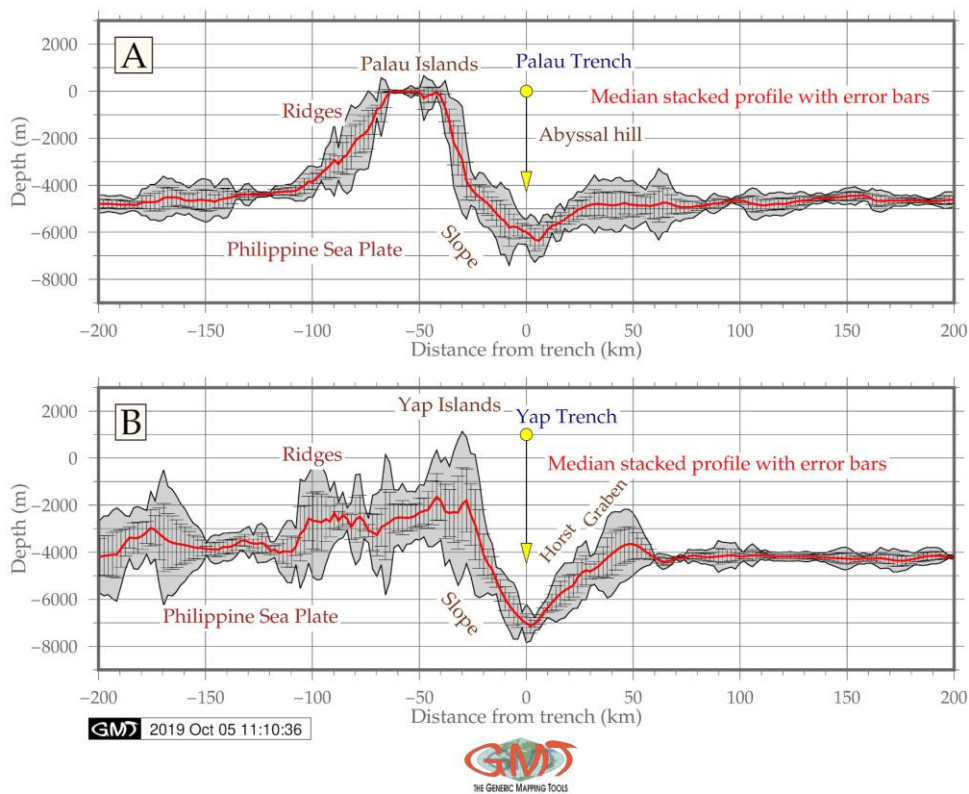


Fig. 7 Geomorphic graph models of the Palau (A) and Yap (B) trenches.  
Figure source: author, made using GMT

### 2.3 Results on statistical analysis

According to the statistical analysis (Fig. 8), the highest values for the Yap Trench are from -4000 m to -4200 m (278 samples) with 19 % and 17 % of the total data pool, respectively. As for the Palau Trench, the data distribution has interesting pattern: the amount of depths in the range of -5000 m to -4000 m is larger comparing to the Yap Trench (737 at Palau Trench versus 605 by Yap). The same situation is for the depth range at -5000 m to -6000 m: the Yap Trench has in total 53 only samples (16+13+11+13) while the Palau Trench has 152 samples (74+41+18+19). However, for the depths over -5000 m, the model of two trenches significantly changes: decreases for the Palau Trench more clearly: the Yap Trench has more deep values within range of -7000 m to -6000 m: 68 observation samples, while the Palau Trench has only 34 samples for the same depths diapason. That means, the Palau Trench has more values higher and/or below -6000 m, but the Yap Trench has dominating depths at deeper values. In general, the Palau Trench has more gentle slope both landwards and oceanwards, while the Yap Trench has steeper slopes and generally deeper sample observation records. Topographic profiles of the Yap Trench axis have very sharp V-shape and more U-shape for the Palau Trench. The V-shaped trench generally indicates bare bottom of the Yap Trench with very thin sediment cover of the axis.

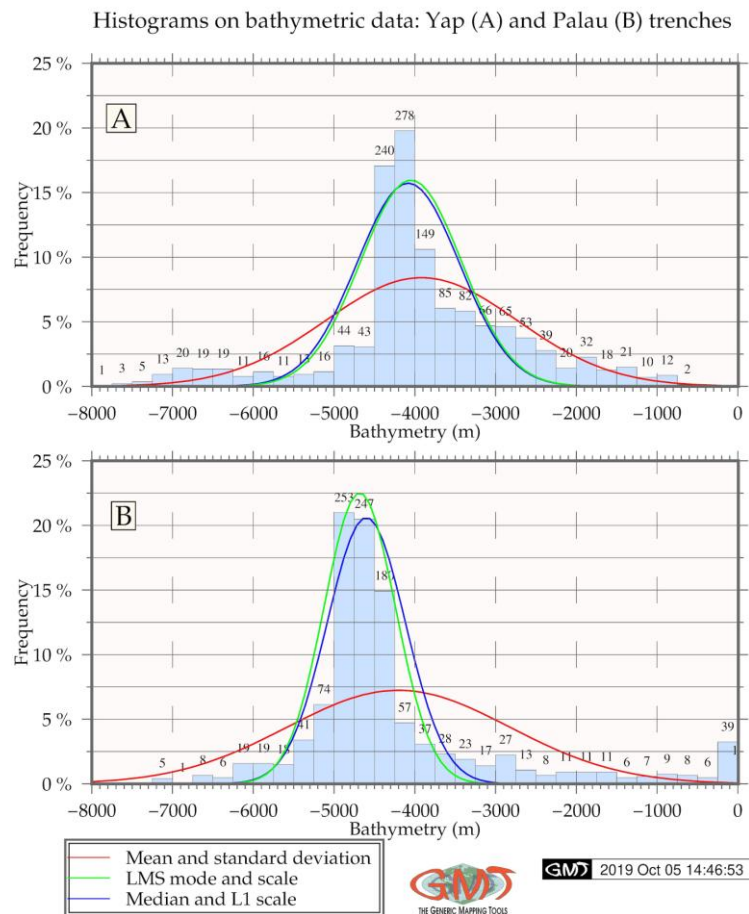


Fig. 8 Statistical histograms of the Yap and Palau trenches: depths distribution.  
Figure source: author, made using GMT

Graph of the modelled trend curves of the Yap Trench geomorphology  
 Fitted regression models  $y=f(x)+e$ , by weighted least squares (WLS), polynomial and Fourier

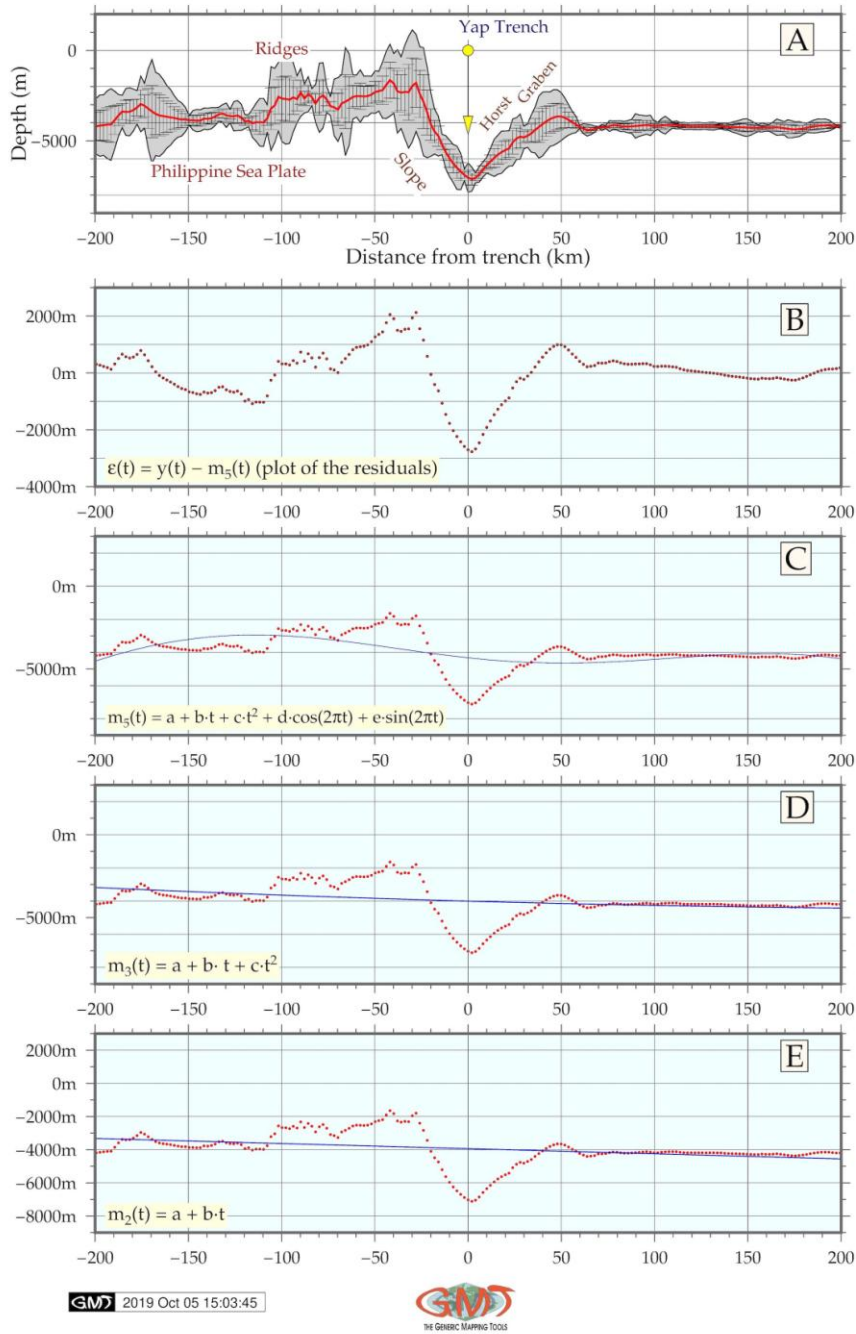


Fig. 9 Modelled trend curves of the gradient slopes: Yap Trench.  
 Figure source: author, made using GMT

Palau Trench geomorphology: graph of the modelled trend curves of the  
 Fitted regression models  $y=f(x)+e$ , by weighted least squares (WLS), polynomial and Fourier

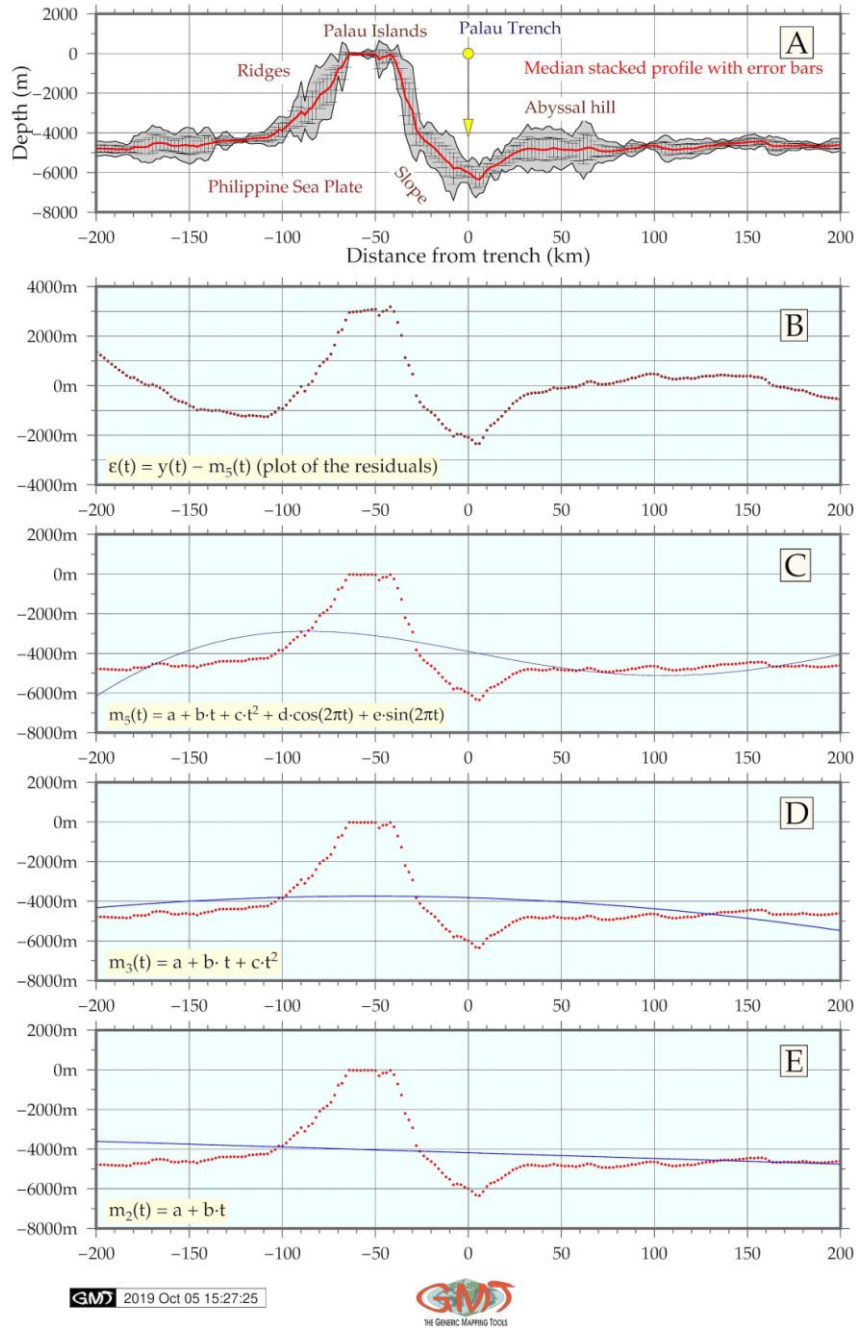


Fig. 10 Modelled trend curves of the gradient slopes: Palau Trench.  
 Figure source: author, made using GMT

## Conclusion

In this study, the GMT based cartographic approach was designed and presented for bathymetric and geomorphic comparative analysis of two hadal trenches, Yap and Palau. The cross-sectional profiles were modelled, visualized, mapped and their values calculated by GMT simulation modules. Technically, modelling included using GMT modules: `grdcut`, `makecpt`, `grdimage`, `psscale`, `grdcontour`, `psbasemap`, `psxy`, `grdtrack`, `convert`, `pstext`, `logo`, `psconvert`. Calculated statistical results were compared for both trenches and trends of their bathymetric shapes are visualized. The statistical values of the geomorphic elevations show variations in the both trenches. As calculated, in general, the Palau Trench has more gentle geomorphic slope land- and oceanwards, while the Yap Trench has steeper slopes and deeper records. Topographic profiles of the axis of the Yap Trench have sharp V-shape while the Palau Trench has U-shape.

The results were compared with previously made research on Yap and Palau trenches. It was seen that barer bottom of the Yap Trench may result from the thin sediment cover of the axis which proves correlation between the factors (geology, geomorphology, geophysics, tectonics, sedimentation) affecting trench structure and dynamics (Yoshida, 2017; Lemenkova, 2018a; Kim et al., 2009). Statistical analysis has a crucial importance for the geospatial data interpretation and modelling. It enables to reveal general trends and helps to highlight correlation in the data distribution. Examples of the data classification through the statistical analysis by data sorting, ordering, clustering and grouping in various aspects of geospatial analysis are reported (Klaučo et al., 2014; Klaučo et al., 2013; Lemenkova, 2019a). Using the statistical analysis in Earth studies was reported in various papers (Roberts et al., 2019; Lemenkova, 2019e).

The data analysis in marine geology can be assessed using various approaches, for examples using GIS, LaTeX graphical plotting, R programming language (Kotov and Pälke, 2019; Lemenkova, 2019c; Lemenkova, 2018b), various statistical libraries of Python language, such as Matplotlib, Seaborn, StatsModels, NumPy, SciPy and Pandas (Seabold and Perktold, 2010; Lemenkova, 2019), using Gretl statistical libraries, combination of ArcGIS, Python, R, MATLAB, and C++ (Roberts et al., 2010), SPSS Statistics and other methods (Borradaile, 2003). The advantage of the GMT consists in some statistical functions and data analysis embedded in the toolset.

## Discussion

The traditional GIS, e.g. ArcGIS, MapInfo, QGIS have been traditionally used in geosciences (e.g. Klaučo et al., 2017; Suetova et al., 2005b) due to availability of the graphical user interface (GUI), available variety of functions for spatial analysis and other features. However, the GMT has more flexibility through its scripting approach and compatibility with UNIX utilities. Combination of ArcGIS with GMT and CARIS bathymetric data processing presents approach to the seafloor mapping (Gauger et al., 2007).

Modelling and visualization in GMT with high resolution of SRTM15\_PLUS grids of 15 arc seconds enable to perform high quality maps as demonstrated in this paper. The SRTM15\_PLUS grid raster tiles proved to be the perfect dataset for the detailed modelling in the submarine topography. The definitive advantage of the GMT consists in its scripting approach: modelling various areas using GMT can be done using available scripts that only requires appropriate adjustment of data, coordinates and cartographic solutions (colour palettes, placements of the elements and annotations) to the regional settings of the study area. Adapting existing GMT scripts can be done for series of thematic maps.

The increasing growth of the machine learning methods and automatization of the data processing promises to facilitate the cartographic routines and makes monotonous work of digitizing more precise, effective and fast. The use of GMT scripting technologies in the automatization of the cross-section transects, as modelling presented in this paper, can be applied for other regions and areas. The paper demonstrates using GMT software to one of the most morphologically rich regions in the Pacific Ocean. It shows how the geomorphic cross-section profile analysis and mapping free-air gravity anomaly can provide insights into properties of studied bathymetric features. The provided scripts make the presented material reproducible and applicable to other locations. Paper brings novel approach in applying automatic cartographical processes to bathymetry data.

*Acknowledgement: This research was funded by the China Scholarship Council (CSC), State Oceanic Administration, Marine Scholarship of China, Grant Nr. 2016SOA002, Beijing, People's Republic of China. I thank two anonymous reviewers for their comments, critics and suggestions that helped to improve the initial manuscript: both text and maps.*

## References

- AGAPOVA, G. V., BUDANOVA, L. Y., ZENKEVICH, N. L., LARINA, N. I., LITVIN, V. M., MAROVA, N. A., RUDENKO, M. V., TURKO, N. N. (1979). *Geomorphology of the Ocean Floor, Geofizika okeana. Geofizika okeanskogo dna*, Moscow (Izd. Nauka), 150-205 (in Russian).
- BECCALUVA, L., SERRI, G., DOSTAL, J. (1986). Geochemistry of Volcanic Rocks from the Mariana and Palau Trenches Bearing on the Tectono-Magmatic Evolution of the Mariana Trench-Arc-Backarc System. *Developments in Geotectonics*, 21, 481-508. DOI: 10.1016/B978-0-444-42688-8.50026-6
- BECKER, J. J., SANDWELL, D. T., SMITH, W. H. F., BRAUD, J., BINDER, B., DEPNER, J., FABRE, D., FACTOR, J., INGALLS, S., KIM, S. H., LADNER, R., MARKS, K., NELSON, S., PHARAOH, A., TRIMMER, R., VON ROSENBERG, J., WALLACE, G., WEATHERALL, P. (2009). Global Bathymetry and Elevation Data at 30 Arc Seconds Resolution: SRTM30\_PLUS. *Marine Geodesy*, 32(4), 355-371.
- BORRADAILE, G. J. (2003). *Statistics of Earth Science Data*. Berlin, New York (Springer), 79.
- CHAPMAN, M. E., BODINE, J. H. (1979). Considerations of the indirect effect in marine gravity modeling. *American Geophysical Union (AGU)*, 84(B8), 3889-3892. DOI: 10.1029/JB084iB08p03889
- DONG, D., ZHANG, Z., BAI, Y., FAN, J., ZHANG, G. (2018). Topographic and sedimentary features in the Yap subduction zone and their implications for the Caroline Ridge subduction. *Tectonophysics*, 722, 410-421. DOI: 10.1016/j.tecto.2017.11.030
- FUJIWARA, T., TAMURA, C., NISHIZAWA, A., FUJIOKA, K., KOBAYASHI, K., IWABUCHI, Y. (2000). Morphology and tectonics of the Yap Trenches. *Marine Geophysical Research*, 21, 69-86.
- GAUGER, S., KUHN, G., GOHL, K., FEIGL, T., LEMENKOVA, P., HILLENBRAND, C. (2007). Swath-bathymetric mapping. In GOHL, K. (ed.) *The expedition Antarktis-XXIII/4 of the Research Vessel 'Polarstern' in 2006. Berichte zur Polar- und Meeresforschung = Reports on Polar and Marine Research*, 557, 38-45. DOI: 10.6084/m9.figshare.7439231 Available at: <https://www.coldregions.org/vufind/Record/288392>
- GEOID & GRAVITY DATASETS (2019). [cit. 2019-12-20]. Available at: <ftp://topex.ucsd.edu/pub>
- GESCH, D., FARR, T. G., SLATER, J., COOK, S. (2006a). New products from the Shuttle Radar Topography Mission. *EOS Transactions, American Geophysical Union*, 87, 174.
- GESCH, D., MULLER, J. P., FARR, T. G. (2006b). The Shuttle Radar Topography Mission – Data validation and applications, foreword to special issue. *Photogrammetric Engineering and Remote Sensing*, 72, 233-234.
- GMT Datasets 2019. [cit. 2019-12-20]. Available at: <http://gmt.soest.hawaii.edu/doc/latest/datasets.html>
- HARRIS, P. T., MACMILLAN-LAWLER, M., RUPP, J., BAKER, E. K. (2014). Geomorphology of the oceans. *Marine Geology*, 352, 4-24. DOI: 10.1016/j.margeo.2014.01.011
- HARRIS, P. T. (2012). Seafloor Geomorphology as Benthic Habitat. 6. Seafloor Geomorphology – Coast, Shelf and Abyss. *GeoHAB Atlas of Seafloor Geomorphic Features and Benthic Habitat*, 109-155. DOI: 10.1016/B978-0-12-385140-6.00006-2
- HAXBY, F., KARNER, G. D., LA BREQUE, J. L., WEISSEL, J. K. (1983). Digital images of combined oceanic and continental data sets and their uses in tectonic studies. *EOS Transactions, American Geophysical Union*, 64, 995-1004.
- IHO, 2008. *Standardization of Undersea Feature Names: Guidelines Proposal form Terminology*, 4th ed. International Hydrographic Organisation and Intergovernmental Oceanographic Commission, Monaco.
- IHO-IOC, 2012. *GEBCO Gazetteer of Undersea Feature Names*, October 2012 version.
- JOSEPH, A. (2017). The Chaotic and Vibrant Seafloor. From Mud Volcanoes to Giant Squid. Chapter 1. In *Investigating Seafloors and Oceans*, 1-79. DOI: 10.1016/B978-0-12-809357-3.00001-1
- KIM, Y. M., LEE, S. M., OKINO, K. (2009). Comparison of gravity anomaly between mature and immature intra-oceanic subduction zones in the western Pacific. *Tectonophysics*, 474, 657-673. DOI: 10.1016/j.tecto.2009.05.004
- KLAUČO, M., GREGOROVÁ, B., STANKOV, U., MARKOVIĆ, V., LEMENKOVA, P. (2013). Determination of ecological significance based on geostatistical assessment: A case study from the Slovak

- Natura 2000 protected area. *Central European Journal of Geosciences*, 5(1), 28-42. DOI: 10.2478/s13533-012-0120-0
- KLAUČO, M., GREGOROVÁ, B., STANKOV, U., MARKOVIĆ, V., LEMENKOVA, P. (2014). Landscape metrics as indicator for ecological significance: assessment of Sitno Natura 2000 sites, Slovakia. In *Ecology and Environmental Protection. Proceedings of International Conference (Belarusian State University, Mar. 19–20, 2014)*. Minsk (BSU Press), 85-90. DOI: 10.6084/m9.figshare.7434200 Available at: <http://elib.bsu.by/handle/123456789/103362>
- KLAUČO, M., GREGOROVÁ, B., STANKOV, U., MARKOVIĆ, V., LEMENKOVA, P. (2017). Land planning as a support for sustainable development based on tourism: A case study of Slovak Rural Region. *Environmental Engineering and Management Journal*, 2(16), 449-458. DOI: 10.30638/eemj.2017.045
- KOBAYASHI, K., FUJIOKA, K., FUJIWARA, T., IWABUCHI, Y., KITAZATO, H. (1997). Why is the Palau Trench so Deep? Deep-Sea Trench without Plate Convergence. *Proceedings of the Japan Academy, Series B*, 73(6), 89-94.
- KOTOV, S., PÁLIKE, H. (2019). Enhanced Principal Tensor Analysis as a tool for 3-way geological data reconstructions. *Computers and Geosciences*, 123, 161-171. DOI: 10.1016/j.cageo.2018.11.001
- KUHN, G., HASS, C., KOBER, M., PETITAT, M., FEIGL, T., HILLENBRAND, C. D., KRUGER, S., FORWICK, M., GAUGER, S., LEMENKOVA, P. (2006). The response of quaternary climatic cycles in the South-East Pacific: development of the opal belt and dynamics behaviour of the West Antarctic ice sheet. In GOHL, K. (ed.) *Expeditionsprogramm Nr.75 ANT XXIII/4, AWI Helmholtz Centre for Polar and Marine Research*, Bremerhaven, Germany. DOI: 10.13140/RG.2.2.11468.87687
- LEE, S. M. (2004). Deformation from the convergence of oceanic lithosphere into Yap trench and its implications for early-stage subduction. *Journal of Geodynamics*, 37, 83-102. DOI:10.1016/j.jog.2003.10.003
- LEMENKOVA, P. (2018a). R scripting libraries for comparative analysis of the correlation methods to identify factors affecting Mariana Trench formation. *Journal of Marine Technology and Environment*, 2, 35-42. DOI: 10.6084/m9.figshare.7434167
- LEMENKOVA, P. (2018b). Factor Analysis by R Programming to Assess Variability Among Environmental Determinants of the Mariana Trench. *Turkish Journal of Maritime and Marine Sciences*, 4, 146-155. DOI: 10.6084/m9.figshare.7358207
- LEMENKOVA, P. (2018c). Hierarchical Cluster Analysis by R language for Pattern Recognition in the Bathymetric Data Frame: a Case Study of the Mariana Trench, Pacific Ocean. In KRASNYANSKY, M. N. (ed.) *Virtual Simulation, Prototyping and Industrial Design. Proceedings of the 5th International Scientific-Practical Conference*, 2(5), Tambov, TSTU Press, 147-152. DOI: 10.6084/m9.figshare.7531550
- LEMENKOVA, P. (2019a). K-means Clustering in R Libraries {cluster} and {factoextra} for Grouping Oceanographic Data. *International Journal of Informatics and Applied Mathematics*, 2(1), 1-26. ISSN: 2667-6990. DOI: 10.6084/m9.figshare.9891203
- LEMENKOVA, P. (2019b). Statistical Analysis of the Mariana Trench Geomorphology Using R Programming Language. *Geodesy and Cartography*, 45 (2), 57-84. ISSN: 2029-6991. DOI: 10.3846/gac.2019.3785
- LEMENKOVA, P. (2019c). An Empirical Study of R Applications for Data Analysis in Marine Geology. *Marine Science and Technology Bulletin*, 8(1), 1-9. ISSN: 2147-9666. DOI: 10.33714/masteb.486678
- LEMENKOVA, P. (2019d). Processing oceanographic data by Python libraries NumPy, SciPy and Pandas. *Aquatic Research*, 2, 73-91. DOI: 10.3153/AR19009
- LEMENKOVA, P. (2019e). Testing Linear Regressions by StatsModel Library of Python for Oceanological Data Interpretation. *Aquatic Sciences and Engineering*, 34, 51-60. DOI: 10.26650/ASE2019547010
- LIU, Y., LIU, X., LV, X., CAO, W., SUN, C, LU, J., WANG, C., LU, B., YANG, J. (2018). Watermass properties and deep currents in the northern Yap Trench T observed by the Submersible Jiaolong system. *Deep-Sea Research Part I*, 139, 27-42. DOI: 10.1016/j.dsr.2018.06.001
- NOAA Documentation (2019). *SRTM15\_PLUS: Data fusion of Shuttle Radar Topography Mission (SRTM) land topography with measured and estimated seafloor topography* (NCEI Accession 0150537) [cit. 2019-12-20]. Available at: <https://data.nodc.noaa.gov/cgi-bin/iso?id=gov.noaa.nodc:0150537>
- ODA, H., SENNA, H. (1994). Regional variation in surface wave group velocities in the Philippine Sea. *Tectonophysics*, 233, 265-277.
- OGUCHI, T. (2019). Geomorphological debates in Japan related to surface processes, tectonics, climate, research principles and international geomorphology. *Geomorphology* (In Press, Corrected Proof) Available online 27 June 2019. DOI: 10.1016/j.geomorph.2019.06.019



- OHARA, Y., FUJIOKA, K., ISHIZUKA, O., ISHII, T. (2002). Peridotites and volcanics from the Yap arc system: implications for tectonics of the southern Philippine Sea Plate. *Chemical Geology*, 189, 35-53.
- OLSON, C. L., BECKER, J. J., SANDWELL, D. T. (2014). A new global bathymetry map at 15 arcsecond resolution for resolving seafloor fabric: SRTM15\_PLUS. *EOS Transactions, American Geophysical Union*, edited, pp. Abstract OS34A-03. [cit. 2019-12-20]. Available at: [ftp://topex.ucsd.edu/pub/srtm15\\_plus/topo15.grd](ftp://topex.ucsd.edu/pub/srtm15_plus/topo15.grd)
- OWEN, L. A. (2013). Tectonic geomorphology: a perspective. In SHRODER, J., OWEN, L. A. (eds.), *Treatise on Geomorphology. Reference Module in Earth Systems and Environmental Sciences*. Academic Press, San Diego, 5, *Tectonic Geomorphology*, 3-12. DOI: 10.1016/B978-0-12-374739-6.00077-4
- PILLET, R., ROULAND, D., ROULT, G., WIENS, D. A. (1999). Crust and upper mantle heterogeneities in the Southwest Pacific from surface wave phase velocity analysis. *Physics of the Earth and Planetary Interiors*, 110, 211-234.
- ROBERTS, J. J., BEST, B. D., DUNN, D. C., TREML, E. A., HALPIN, P. N. (2010). Marine geo-spatial ecology tools: an integrated framework for ecological geoprocessing with ArcGIS, Python, R, MATLAB, and C++. *Environmental Modelling and Software*, 25, 1197-1207, DOI: 10.1016/j.envsoft.2010.03.029
- ROBERTS, N. M., TIKOFF, B., DAVIS, J. R., STETSON-LEE, T. (2019). The utility of statistical analysis in structural geology. *Journal of Structural Geology*, 125, 64-73.
- SATO, T., KASAHARA, J., KATAO, H., TOMIYAMA, N., MOCHIZUKI, K., KORESAWA, S. (1997). Seismic observations at the Yap Islands and the northern Yap Trench. *Tectonophysics*, 271, 285-294.
- SCRIPPS INSTITUTION OF OCEANOGRAPHY, SATELLITE GROUP (2019). [cit. 2019-12-20]. Available at: [https://topex.ucsd.edu/WWW\\_html/srtm15\\_plus.html](https://topex.ucsd.edu/WWW_html/srtm15_plus.html)
- SCHENKE, H. W., LEMENKOVA, P. (2008). Zur Frage der Meeresboden-Kartographie: Die Nutzung von AutoTrace Digitizer für die Vektorisierung der Bathymetrischen Daten in der Petschora-See. *Hydrographische Nachrichten*, 25(81), 16-21. DOI: 10.6084/m9.figshare.7435538.v2
- SEABOLD, S., PERKTOLD, J. (2010). Statsmodels: Econometric and statistical modeling with Python. In *Proceedings of the 9th Python in Science Conference*, 1-6.
- SETON, M., MÜLLER, R. D., ZAHIROVIC, S., GAINA, C., TORSVIK, T., SHEPHARD, G., TALSMA, A., GURNIS, M., TURNER, M., MAUS, S., CHANDLER, M. (2012). Global continental and ocean basin reconstructions since 200 Ma. *Earth-Science Review*, 113, 212-270. DOI: 10.1016/j.earscirev.2012.03.002
- SMITH, W. H. F., SANDWELL, D. T. (1995). Marine gravity field from declassified Geosat and ERS-1 altimetry. *EOS Transactions, American Geophysical Union*, 76, Fall Mtng Suppl, F156.
- SMITH, W. H. F. (1993). On the accuracy of digital bathymetric data. *Journal of Geophysical Research*, 98 (B6): 9591-9603.
- SRTM15\_PLUS DATASET (2019). [cit. 2019-12-20]. Available at: [ftp://topex.ucsd.edu/pub/srtm15\\_plus/topo15.grd](ftp://topex.ucsd.edu/pub/srtm15_plus/topo15.grd)
- SUETOVA, I. A., USHAKOVA, L. A., LEMENKOVA, P. (2005a). Geoinformation mapping of the Barents and Pechora Seas. *Geography and Natural Resources*, 4, 138-142. DOI: 10.6084/m9.figshare.7435535
- SUETOVA, I., USHAKOVA, L., LEMENKOVA, P. (2005b). Geoecological Mapping of the Barents Sea Using GIS. In *Digital Cartography & GIS for Sustainable Development of Territories. Proc. International Cartographic Conference ICC. July 9-16, La Coruña, España*. DOI:10.6084/m9.figshare.7435529
- TSUBOI, T., WADA, H., NAKAMURA, T., HANG, T. T., MATSUZAKI, H., OTSUJI, N., FUJIOKA, K., OGURI, K., KITAZATO, H. (2014). Deep-sea limestone block as a source of 14C-depleted dissolved inorganic carbon at the Palau Trench. *Chemical Geology*, 364, 1-8.
- WESSEL, P., WATTS, A. B. (1988). On the accuracy of marine gravity measurements. *Journal of Geophysical Research*, 93, 393-413.
- WESSEL, P., SMITH, W. H. F. (1996). A Global Self-consistent, Hierarchical, High-resolution Shoreline Database. *Journal of Geophysical Research*, 101, 8741-8743.
- XU, W., GAO, Y. H., GONG, L. F., LI, M., PANG, K. L., LUO, Z. H. (2019). Fungal diversity in the deep-sea hadal sediments of the Yap Trench by T cultivation and high throughput sequencing methods based on ITS rRNA gene. *Deep-Sea Research Part I*, 145, 125-136.
- YANG, J., CUI, Z., DADA, O. A., YANG, Y., YU, H., XU, Y., LIN, Z., CHEN, Y., TANG, X. (2018). Distribution and enrichment of trace metals in surface marine sediments T collected by the manned sub-

- mersible Jiaolong in the Yap Trench, northwest Pacific Ocean. *Marine Pollution Bulletin*, 135, 1035-1041. DOI: 10.1016/j.marpolbul.2018.08.038
- YEH, Y. L., KAO, H., WEN, S., CHANG, W. Y., CHEN, C. H. (2013). Surface wave tomography and azimuthal anisotropy of the Philippine Sea Plate. *Tectonophysics*, 592, 94-112. DOI: 10.1016/j.tecto.2013.02.005
- YOSHIDA, M. (2017). Trench dynamics: Effects of dynamically migrating trench on subducting slab morphology and characteristics of subduction zones systems. *Physics of the Earth and Planetary Interiors*, 268, 35-53.

## R e s u m é

### **Automatické spracovanie dát na vizualizáciu hlbokomorských priekop Yap a Palau s použitím Generic Mapping Tools**

Táto práca prezentuje skúsenosti s použitím Generic Mapping Tools (GMT) – kartografických skriptovacích nástrojov na spracovanie dát. Výskumnú oblasť tvorili priekopy Yap (YT) a Palau (PT) – hlbokomorské oceánske priekopy nachádzajúce sa v juhozápadnej časti Tichého oceánu. Metodika zahŕňala tieto kroky:

- extrahovanie rastrových dát v sieti SRTM15\_plus,
- tematické mapovanie vizualizujúce topografické a geologické pomery,
- modelovanie geoidu, gravitačné modelovanie a mapovanie,
- geomorfologické modelovanie pomocou automatizovanej digitalizácie priečných profilov vybraných segmentov oboch priekop,
- štatistické analýzy a grafy ilustrujúce distribúciu dát – frekvenciu distribúcie hĺbok,
- vykreslenie trendových kriviek gradientov sklonov modelované pomocou troch matematických aproximácií znázorňujúce rozdiely v strmosti sklonov oboch priekop.

Výsledky zahŕňajú ukážky odlišností hĺbok a porovnanie oboch priekop: hĺbka YT dosahuje -7 000 m, zatiaľ čo PT je všeobecne plytšia a dosahuje -6 200 m. YT má prudšie sklony a strmší gradient profilu smerom k oceánu v porovnaní s PT. V rozmedzí od -7 000 m do -6 000 m v YT sa urobilo 68 vzoriek meraní, zatiaľ čo PT 34 meraní. PT má viac vzoriek pod -6 000 m, ale v YT dominujú väčšie hĺbky. Všeobecne má PT geomorfologicky miernejšie sa zvažujúce sklony smerom od pevniny a ďalej na juh, YT má strmšie sklony a väčšie hodnoty hĺbok. Priečný profil YT má ostrý tvar písmena V, zatiaľ čo PT má tvar písmena U. To naznačuje obnaženejšie dno YT s veľmi tenkým sedimentárnym pokryvom.

Rýchly rozvoj metód strojového učenia zdôrazňuje dôležitosť automatizovaného spracovania geodát. Opísaná automatizovaná tvorba priečných profilov pomocou GMT je presnejšia, rýchlejšia a menej náchylná na chyby v porovnaní s manuálnym procesom modelovania v prostredí programov geografických informačných systémov (GIS). Prezentovaná práca prispieva k rozvoju kartografických metodík, ktoré môžu nájsť uplatnenie v podobne zameraných štúdiách.

- Obr. 1. Topografická mapa študovaných oblastí Filipínskeho mora, priekopa Yap a Palau
- Obr. 2. Mapa geologických a tektonických pomerov priekop
- Obr. 3. Mapa gravitačných anomálií priekop
- Obr. 4. Mapa modelu geoidu priekop
- Obr. 5. Geomorfologický model 3D priekop
- Obr. 6. Mapa digitalizovaných priečných profilov priekop
- Obr. 7. Geomorfologické modely priekop
- Obr. 8. Histogramy hĺbok priekop
- Obr. 9. Trendové modely kriviek gradientov sklonu priekopy Yap
- Obr. 10. Trendové modely kriviek gradientov sklonu priekopy Palau

Prijaté do redakcie: 26. októbra 2019

Zaradené do tlače: december 2019